

Multiredox Active [3 × 3] Copper Grids

Hiroki Sato, Lisa Miya, Kiyotaka Mitsumoto, Takuto Matsumoto, Takuya Shiga, Graham N. Newton, and Hiroki Oshio*

Graduate School of Pure and Applied Sciences, University of Tsukuba, Tennodai 1-1-1, Tsukuba, Ibaraki 305-8571, Japan

Supporting Information

ABSTRACT: A nonanuclear copper grid complex, $[\text{Cu}^{\text{II}}_9(\text{L})_6](\text{BF}_4)_6 \cdot 1\text{-PrOH} \cdot 5\text{H}_2\text{O}$ ($1 \cdot 1\text{-PrOH} \cdot 5\text{H}_2\text{O}$; $\text{L} = 2,6\text{-bis}[5\text{-}(2\text{-pyridinyl})\text{-}1\text{H-pyrazol-}3\text{-yl}]\text{pyridine}$), was synthesized with a [3 × 3] grid structure consisting of nine Cu^{II} ions and six deprotonated ligands and displayed four-step quasi-reversible redox behavior from $[\text{Cu}^{\text{II}}_9]$ to $[\text{Cu}^{\text{I}}_4\text{Cu}^{\text{II}}_5]$. The corresponding heterovalent complex $[\text{Cu}^{\text{I}}_2\text{Cu}^{\text{II}}_7(\text{L})_6](\text{PF}_6)_4 \cdot 3\text{H}_2\text{O}$ ($2 \cdot 3\text{H}_2\text{O}$) was successfully isolated and had a distorted core structure that radically changed the intramolecular magnetic coupling pathways.

Polynuclear molecular cluster systems with physical properties that can be altered upon the application of external stimuli such as temperature, light, electric field, and external magnetic field have attracted great attention because of their potential to function as molecular devices in future technologies.¹ The electronic states of transition-metal ions and the interactions between neighboring centers can also be affected by external stimuli. Multinuclear systems with dynamic physical properties are therefore highly sought-after as useful molecular units. To date, we have searched for clusters that display switchable behavior as candidates for multistable molecular components and have reported several square-type and grid complexes derived from polypyridine multidentate planar ligands.² In these molecular systems, multiredox processes and spin-transition phenomena were investigated. In attempts to design molecular devices, the use of multidentate ligands is an excellent tactic because desirable polynuclear systems with regular arrays of metal ions can be designed and synthesized with a degree of confidence. Grid-type complexes are a good example of the artificial alignment of metal ions,³ and Lehn and co-workers were pioneers in the research of such species, reporting many $[n \times n]$ grids,⁴ including a tetranuclear iron(II) multistep spin-crossover (SCO) grid complex.⁵ Thompson et al. also investigated magnetic grid-type clusters using flexible amide ligands,⁶ and recently Mayer et al. and Sato et al. reported multistep iron(II) SCO grids.⁷ Tong et al. reported the synthesis and magnetic properties of heterometal grids,⁸ while Hou et al. studied the ion-sensing and metal-exchange properties of copper grids.⁹

Grid complexes can have many stable states because of the large number of metal ions, each of which has the potential to change the electronic state. The generation of multinuclear clusters in which the ions are held in a range of different coordination environments means that the different metal centers are likely to exhibit contrasting electronic properties. Thus, the development of new grid-type complexes is an

important area of research. We synthesized two nonanuclear [3 × 3] grid-type copper complexes supported by the multidentate ligand 2,6-bis[5-(2-pyridinyl)-1H-pyrazol-3-yl]pyridine (H_2L ; Scheme S1 in the Supporting Information, SI). Their structures and magnetic and electrochemical properties were investigated and are discussed herein.

The reaction of $\text{Cu}(\text{BF}_4)_2 \cdot n\text{H}_2\text{O}$ with H_2L and Et_3N in a 1-propanol/acetonitrile solution (3:7) yielded a nonanuclear $\{\text{Cu}^{\text{II}}_9\}$ complex, $[\text{Cu}^{\text{II}}_9(\text{L})_6](\text{BF}_4)_6 \cdot 3\text{CH}_3\text{CN} \cdot 1\text{-PrOH} \cdot 13\text{H}_2\text{O}$ ($1 \cdot 3\text{CH}_3\text{CN} \cdot 1\text{-PrOH} \cdot 13\text{H}_2\text{O}$).¹⁰ A mixed-valence nonanuclear $\{\text{Cu}^{\text{I}}_2\text{Cu}^{\text{II}}_7\}$ complex, $[\text{Cu}^{\text{I}}_2\text{Cu}^{\text{II}}_7(\text{L})_6](\text{PF}_6)_4 \cdot 4\text{CH}_3\text{CN} \cdot 2\text{CH}_3\text{OH} \cdot 2\text{H}_2\text{O}$ ($2 \cdot 4\text{CH}_3\text{CN} \cdot 2\text{CH}_3\text{OH} \cdot 2\text{H}_2\text{O}$), was prepared by the reaction of $[\text{Cu}(\text{CH}_3\text{CN})_4](\text{BF}_4)$ ¹¹ with H_2L , Et_3N , and NH_4PF_6 in methanol/acetonitrile under a nitrogen atmosphere.¹²

Single-crystal X-ray structural analyses reveal that $1 \cdot 3\text{CH}_3\text{CN} \cdot 1\text{-PrOH} \cdot 13\text{H}_2\text{O}$ and $2 \cdot 4\text{CH}_3\text{CN} \cdot 2\text{CH}_3\text{OH} \cdot 2\text{H}_2\text{O}$ have similar [3 × 3] grid-like structures, composed of six ligands and nine copper ions (Figure 1).^{13,14} In this [3 × 3] grid structure, there

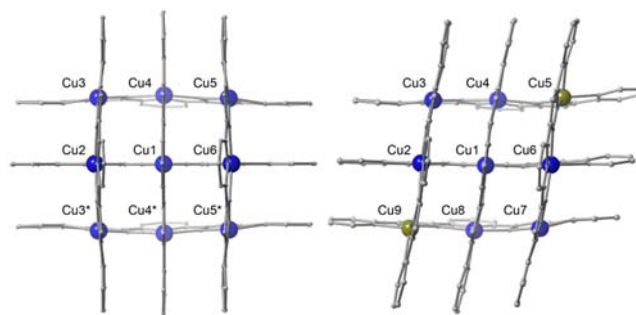


Figure 1. Crystal structures of **1** (left) and **2** (right). Counterions and solvent molecules were omitted for clarity. Color code: C, gray; N, light blue; Cu^{II} , blue; Cu^{I} , khaki.

are three different classes of coordination sites, which can be categorized as central, edge, and corner positions. The central copper ion has an octahedral coordination geometry with six nitrogen atoms coordinating from two tridentate ligand sites. The copper ions on the edges have square-pyramidal coordination environments with one tridentate and one bidentate ligand sites, while the corner ions are coordinated by two bidentate sites in a highly distorted tetrahedral manner. Bond-valence-sum calculations¹⁵ and charge-balance consider-

Received: June 9, 2013

Published: August 9, 2013

ations conclude that **1** and **2** form $\{\text{Cu}^{\text{II}}_9\}$ and $\{\text{Cu}^{\text{I}}_2\text{Cu}^{\text{II}}_7\}$ grids, respectively.

The overall grid shapes of **1** and **2** are substantially different, with **1** possessing a regular square framework and **2** a distorted rhombic structure (Figure 2). The distortion originates from the

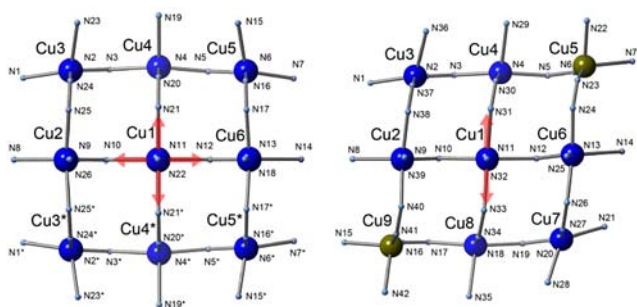


Figure 2. Core structures of **1** (left) and **2** (right). Symmetry operation code *: $x, -y, z$. Red arrows indicate the orientation of the fully occupied $d\sigma$ orbitals of the central ion.

corner copper sites. The four ions in **1** have similar geometries, while the neighboring corner sites in **2** show different levels of distortion, as reflected by their τ_4 parameters.¹⁶ In **1**, all τ_4 values are 0.60, while those in **2** range from 0.49 to 0.63; $\tau_4 = 0.56$ for Cu3, 0.63 for Cu5, 0.49 for Cu7, and 0.62 for Cu9. The τ_4 values in **2** suggest that Cu5 and Cu9 are broadly tetrahedral, while Cu3 and Cu7 are more square-planar in character. The coordination bond lengths of Cu3 and Cu7 are shorter than those of Cu5 and Cu9. These facts imply that Cu5 and Cu9 are monovalent ions. Distortion of the overall square shape induces distortion of the coordination geometry of the central copper ion. In **1**, Cu1 has a compressed-type Jahn–Teller distortion along its bonds with the pyridine groups (N11 and N22) of the two central ligands. On the other hand, the Cu1 ion of **2** has an elongated Jahn–Teller distortion along its bonds with the pyrazolate groups (N31 and N33) of one ligand. Changing the electronic states of the corner ions appears to induce a change in the Jahn–Teller distortions of **1** and **2**.

Magnetic susceptibilities of **1**·1-PrOH·5H₂O and **2**·3H₂O were collected in the temperature range of 1.8–300 K (Figure 3). The $\chi_m T$ values for **1** and **2** at 300 K were 3.37 and 3.10 emu mol⁻¹ K, which were close to the expected values (3.38 and 2.63

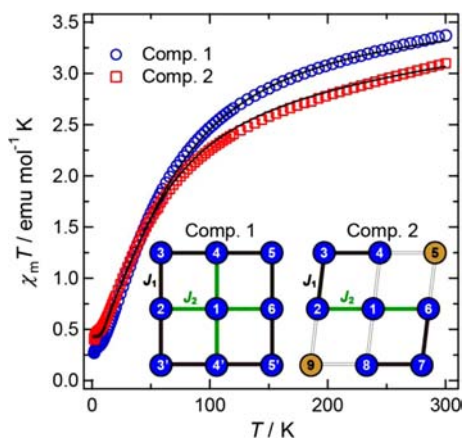


Figure 3. Magnetic susceptibilities of **1**·1-PrOH·5H₂O (○) and **2**·3H₂O (□) with fitting curves (see the text). Inset: schematic spin models. Blue and khaki circles represent Cu^{II} and Cu^I ions, respectively.

emu mol⁻¹ K for $g = 2.0$) of nine and seven magnetically isolated Cu^{II} ions, respectively. As the temperature was lowered, the $\chi_m T$ values decreased, reaching 0.27 and 0.40 emu mol⁻¹ K at 1.8 K, respectively. The temperature dependence of both samples implied that antiferromagnetic interactions were dominant between neighboring Cu^{II} ions. According to the molecular structures, the spin models shown in Figure 3, inset, were applied to the magnetic analyses.¹⁷ The resulting fitting parameters for **1** were $g = 2.12$, $J_1 = -48$ K, and $J_2 = 0$ K, in which J_2 is fixed to zero because of the complete nonoverlap of magnetic orbitals. In general, Cu^{II} ions with compressed Jahn–Teller distortion have an unpaired electron in the d_{z^2} orbital.¹⁸ In **1**, the magnetic path defined as J_2 relates to the interaction between the equatorial ($d_{x^2-y^2}$) orbital of a Jahn–Teller compressed Cu^{II} ion (Cu1) and the Jahn–Teller elongated axial (d_{z^2}) orbital of the edge Cu^{II} ions. The interacting orbitals are fully occupied, and thus J_2 should be negligible and **1** can be considered simply as an antiferromagnetic ring system surrounding a paramagnetic Cu^{II} ion. The best-fit parameters for **2** were $g = 2.16$, $J_1 = -40$ K, and $J_2 = -10$ K. In this case, J_2 is non-negligible because magnetic interactions between the equatorial plane of an elongated Cu^{II} ion (Cu1) and the axial orbital of elongated edge Cu^{II} ions (Cu2 and Cu6) are operative. The J_1 value is of order similar to that of **1** because of the similarity of the magnetic interaction paths. The contrasting structural distortion means that **2** can be considered as an antiferromagnetic chain fragment.

Cyclic voltammetry (CV) measurements of **1** and **2** were conducted in dichloromethane solutions (Figures 4 and S1 in the

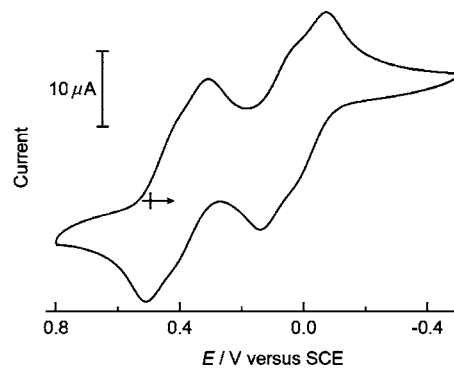


Figure 4. CV data of **1** in $n\text{Bu}_4\text{NPF}_6/\text{CH}_2\text{Cl}_2$. Reference electrode: SCE. Working electrode: Pt. Counter electrode: GC.

SI), and both showed quasi-reversible four-step redox behavior, summarized in Table S1 in the SI. In the CV data of **1** and **2**, the redox potentials of Cu^I/Cu^{II} are similar, implying that the structures of **1** and **2** are the same as those in the solution state. The open-circuit potentials of **1** and **2** were 0.50 and 0.15 V, respectively, suggesting that **2** is the two-electron-reduced species of **1**. Coulometry measurements of **1** and **2** were performed (Figures S2–S4 in the SI). In **1**, electrolysis at -0.50 V corresponds to four-electron reduction. In **2**, electrolyses at -0.50 and $+0.80$ V correspond to two-electron reduction and oxidation processes, respectively. The CV data suggest that the two-electron-reduced species, corresponding to the electronic state of complex **2**, is well-stabilized with comproportionation constant $K_c = 1.8 \times 10^4$ (see the SI). The observation of four reversible one-electron redox processes implies the existence of electronic interactions between neighboring ions.

In summary, two grid-type nonanuclear copper complexes, $\{\text{Cu}^{\text{II}}_9\}$ (**1**) and $\{\text{Cu}^{\text{I}}_2\text{Cu}^{\text{II}}_7\}$ (**2**), were synthesized using the

multidentate polypyridine ligand H₂L. Both compounds have similar [3 × 3] grid structures, but the distortion of the grids is different. The Jahn–Teller distortions of the central Cu^{II} ions of **1** and **2** differ because of the differences in the shape of the grid. The overall magnetic interactions can be explained by considering the effective magnetic orbitals based on the electronic configurations of Jahn–Teller distorted Cu^{II} centers. The electrochemical properties of **1** and **2** were investigated by CV and coulometry, and both showed four-step reversible redox behavior. The [3 × 3] grid-type copper complexes can be considered to be electrochemically and structurally changeable molecular units, a desirable characteristic for the development of molecular devices. To extend this work, we are attempting to synthesize heterometallic grid compounds with bistable physical properties.

■ ASSOCIATED CONTENT

📄 Supporting Information

X-ray crystallographic data in CIF format, ligand structure, spin Hamiltonians used in the magnetism analyses, cyclic voltammogram of **2**, coulometry of **1** and **2**, and K_c calculations. This material is available free of charge via the Internet at <http://pubs.acs.org>. CCDC 930412 and 930413 contain the supplementary crystallographic data for **1** and **2** and can also be obtained free of charge from the Cambridge Crystallographic Data Centre via www.ccdc.cam.ac.uk/data_request/cif.

■ AUTHOR INFORMATION

Corresponding Author

*E-mail: oshio@chem.tsukuba.ac.jp.

Notes

The authors declare no competing financial interest.

■ ACKNOWLEDGMENTS

We gratefully acknowledge a Grant-in-Aid for Scientific Research and for Priority Area “Coordination Programming” (Area 2107) from MEXT of Japan.

■ REFERENCES

- (1) (a) Green, J. E.; Choi, J. W.; Boukai, A.; Bunimovich, Y.; Johnston-Halperin, E.; DeIonno, E.; Luo, Y.; Sheriff, B. A.; Xu, K.; Shin, Y. S.; Tseng, H.-R.; Stoddart, J. F.; Heath, J. R. *Nature* **2007**, *445*, 414. (b) Kay, E. R.; Leigh, D. A.; Zerbetto, F. *Angew. Chem., Int. Ed.* **2007**, *46*, 72. (c) Lent, C. S. *Science* **2000**, *288*, 1597. (d) Sato, O.; Tao, J.; Zhang, Y.-Z. *Angew. Chem., Int. Ed.* **2007**, *46*, 2152. (e) Newton, G. N.; Nihei, M.; Oshio, H. *Eur. J. Inorg. Chem.* **2011**, 3031. (f) Timco, G. A.; Carretta, S.; Troiani, F.; Tuna, F.; Pritchard, R. J.; Murny, C. A.; McInnes, E. J. L.; Ghirri, A.; Candini, A.; Santini, P.; Amoretti, G.; Affronte, M.; Winpenny, R. E. P. *Nat. Nanotechnol.* **2009**, *4*, 173.
- (2) (a) Shiga, T.; Matsumoto, T.; Noguchi, M.; Onuki, T.; Hoshino, N.; Newton, G. N.; Nakano, M.; Oshio, H. *Chem.—Asian J.* **2009**, *4*, 1660. (b) Newton, G. N.; Onuki, T.; Shiga, T.; Noguchi, M.; Matsumoto, T.; Mathieson, J. S.; Nihei, M.; Cronin, L.; Oshio, H. *Angew. Chem., Int. Ed.* **2011**, *50*, 4844.
- (3) Grid review: (a) Ruben, M.; Rojo, J.; Romero-Salguero, F. J.; Uppadine, L. H.; Lehn, J.-M. *Angew. Chem., Int. Ed.* **2004**, *43*, 3644. (b) Thompson, L. K.; Waldmann, O.; Xu, Z. *Coord. Chem. Rev.* **2005**, *249*, 2677. (c) Dawe, L. N.; Shuvaev, K. V.; Thompson, L. K. *Chem. Soc. Rev.* **2009**, *38*, 2334.
- (4) (a) Hanan, G. S.; Volkmer, D.; Schubert, U. S.; Lehn, J.-M.; Baum, G.; Fenske, D. *Angew. Chem., Int. Ed. Engl.* **1997**, *36*, 1842. (b) Ruben, M.; Breuning, E.; Barboiu, E.; Gisselbrecht, J.-P.; Lehn, J.-M. *Chem.—Eur. J.* **2003**, *9*, 291. (c) Stefankiewicz, A. R.; Rogez, G.; Harrowfield, J.; Sobolev, A. N.; Madalan, A.; Huuskonen, J.; Rissanen, K.; Lehn, J.-M. *Dalton Trans.* **2012**, *41*, 13848.
- (5) Ruben, M.; Breuning, E.; Lehn, J.-M.; Ksenofontov, V.; Renz, F.; Güttlich, P.; Vaughan, G. *Chem.—Eur. J.* **2003**, *9*, 4422.
- (6) (a) Anwar, M. U.; Thompson, L. K.; Dawe, L. N.; Habib, F.; Murugesu, M. *Chem. Commun.* **2012**, *48*, 4576. (b) Anwar, M. U.; Shuvaev, K. V.; Dawe, L. N.; Thompson, L. K. *Inorg. Chem.* **2011**, *50*, 12141.
- (7) (a) Schneider, B.; Demeshko, S.; Dechert, S.; Meyer, F. *Angew. Chem., Int. Ed.* **2010**, *49*, 9274. (b) Wu, D.-Y.; Sato, O.; Einaga, Y.; Duan, C.-Y. *Angew. Chem., Int. Ed.* **2009**, *48*, 1475.
- (8) Bao, X.; Liu, W.; Mao, L.-L.; Jiang, S.-D.; Liu, J.-L.; Chen, Y.-C.; Tong, M.-L. *Inorg. Chem.* **2013**, *52*, 6233.
- (9) Han, Y.; Chilton, N. F.; Li, M.; Huang, C.; Xu, H.; Hou, H.; Moubaraki, B.; Langley, S. K.; Batten, S. R.; Fan, Y.; Murray, K. S. *Chem.—Eur. J.* **2013**, *19*, 6321.
- (10) Synthesis of **1**: To a solution of Cu(BF₄)₂·nH₂O (0.09 mmol, 28.7 mg) in 1-PrOH (1.5 mL) was added a mixture of H₂L (0.06 mmol, 22.3 mg) and triethylamine (0.095 mmol, 13.3 μL) in 1-PrOH (1.5 mL). The green suspension reaction mixture was stirred for 20 min. After the addition of acetonitrile (7 mL), the green suspension became a clear green solution. The resulting solution was filtered and left to stand for a few days, after which green lozenge crystals of 1·3CH₃CN·1-PrOH·13H₂O were obtained and dried at ambient temperature (yield 20%). Anal. Calcd for C₁₂₉H₉₆N₄₂B₆F₂₄O₅Cu₉ (1·1-PrOH·5H₂O): C, 45.26; H, 2.83; N, 17.19. Found: C, 45.08; H, 2.27; N, 17.19. IR (KBr pellet, cm⁻¹): 3425.3, 1608.5, 1564.2, 1440.7, 1326.9, 781.1, 1037.6, 1083.9.
- (11) Kubas, G. J. *Inorg. Synth.* **1979**, *19*, 90.
- (12) Synthesis of **2**: Under strict anaerobic conditions, to a solution of Cu(BF₄)₂·nH₂O (0.09 mmol, 28.7 mg) and [Cu^I(CH₃CN)₄](BF₄) (0.30 mmol, 95.9 mg) in CH₃OH (25 mL) was added a mixture of H₂L (0.40 mmol, 146.2 mg) and triethylamine (0.80 mmol, 111.5 μL) in CH₃OH (25 mL). After the addition of acetonitrile (25 mL) to the stirred mixture, a dark-yellowish-green solution was obtained. NH₄PF₆ (3.0 mmol 489 mg) was added to the solution, and the resulting solution was allowed to stand at 40 °C. Brown lozenge crystals of 2·4CH₃CN·2CH₃OH·2H₂O were obtained after a few days, collected by suction filtration, and air-dried (yield 15%). Anal. Calcd for C₁₂₆H₈₄N₄₂P₄F₂₄O₃Cu₉ (2·3H₂O): C, 44.69; H, 2.50; N, 17.37. Found: C, 44.67; H, 2.66; N, 17.37. IR (KBr pellet, cm⁻¹): 3447.5, 1600.8, 1565.1, 1437.8, 1327.9, 773.4, 845.7.
- (13) Crystal data for **1**: C₁₃₅H₇₈N₄₅B₆F₂₄O₁₄Cu₉, $M_r = 3647.14$, monoclinic, $C2/m$, $a = 28.890(2)$ Å, $b = 20.0394(16)$ Å, $c = 25.453(2)$ Å, $\beta = 94.5490(10)^\circ$, $V = 14689(2)$ Å³, $Z = 4$, $D_c = 1.649$ g cm⁻³, $\mu = 1.384$ mm⁻¹, $F(000) = 7288$, and GOF = 1.070. Of a total of 45543 reflections collected, 16895 are unique ($R_{int} = 0.0429$). $R1/wR2 = 0.0827/0.2375$ for 16895 reflections and 1119 parameters [$I > 2\sigma(I)$].
- (14) Crystal data for **2**: C₁₃₆H₉₀N₄₆F₂₄O₄P₄Cu₉, $M_r = 3584.28$, monoclinic, $P2_1/c$, $a = 28.489(10)$ Å, $b = 17.429(6)$ Å, $c = 30.812(11)$ Å, $\beta = 113.184(5)^\circ$, $V = 14064(8)$ Å³, $Z = 4$, $D_c = 1.693$ g cm⁻³, $\mu = 1.483$ mm⁻¹, $F(000) = 7188$, and GOF = 1.062. Of a total of 57019 reflections collected, 20494 are unique ($R_{int} = 0.1212$). $R1/wR2 = 0.0814/0.1887$ for 20494 reflections and 2118 parameters [$I > 2\sigma(I)$].
- (15) Bond valence sum of **1**: Cu1 for 2+, 2.23; Cu2 for 2+, 2.07; Cu3 for 2+, 2.10; Cu4 for 2+, 2.09; Cu5 for 2+, 2.03; Cu6 for 2+, 2.08. Bond valence sum of **2**: Cu1 for 2+, 2.28; Cu2 for 2+, 2.10; Cu3 for 2+, 2.09; Cu4 for 2+, 2.13; Cu5 for 1+, 1.40; Cu6 for 2+, 2.13; Cu7 for 2+, 2.17; Cu8 for 2+, 2.10; Cu9 for 1+, 1.43.
- (16) $\tau_4 = [360 - (\alpha + \beta)]/141$, where α and β are the two largest θ angles in a four-coordinate species, with $\tau_4 = 1$ a perfect tetrahedron and $\tau_4 = 0$ a perfect square-planar geometry. Yang, L.; Powell, D. R.; Houser, R. P. *Dalton Trans.* **2007**, 955.
- (17) Borrás-Almenar, J. J.; Clemente-Juan, J. M.; Coronado, E.; Tsukerblat, B. S. *J. Comput. Chem.* **2001**, *22*, 985.
- (18) (a) Halcrow, M. A. *Chem. Soc. Rev.* **2013**, *42*, 1784. (b) Solanki, N. K.; McInnes, E. J. L.; Mabbs, F. E.; Radojevic, S.; McPartlin, M.; Feeder, N.; Davies, J. E.; Halcrow, M. A. *Angew. Chem., Int. Ed.* **1998**, *37*, 2221. (c) Bridgeman, A. J.; Halcrow, M. A.; Jones, M.; Krausz, E.; Solanki, N. K. *Chem. Phys. Lett.* **1999**, *314*, 176.